Journal of Catalysis 264 (2009) 11–14

Contents lists available at ScienceDirect

Journal of Catalysis

journal homepage: www.elsevier.com/locate/jcat

Priority Communication

Quantification of enhanced acid site accessibility in hierarchical zeolites – The accessibility index

Frédéric Thibault-Starzyk [a,*], Irina Stan [a], Sònia Abelló [b], Adriana Bonilla [b], Karine Thomas [a], Christian Fernandez [a], Jean-Pierre Gilson [a], Javier Pérez-Ramírez [b,c,*]

[a] Laboratoire Catalyse et Spectrochimie, ENSICAEN, Université de Caen, CNRS, 6 Bd du Maréchal Juin, 14050 Caen, France
[b] Institute of Chemical Research of Catalonia (ICIQ), Avinguda Països Catalans 16, 43007 Tarragona, Spain
[c] Catalan Institution for Research and Advanced Studies (ICREA), Passeig Lluís Companys 23, 08010, Barcelona, Spain

ARTICLE INFO

Article history:
Received 8 January 2009
Revised 21 February 2009
Accepted 8 March 2009
Available online 17 April 2009

Keywords:
Accessibility index
Hierarchical zeolites
Desilication
Mesoporous crystals
Infrared spectroscopy
Alkylpyridines
Catalyst effectiveness

ABSTRACT

An accessibility index (ACI) was derived from infrared spectroscopy of substituted alkylpyridines with different size (pyridine: 0.57 nm, 2,6-lutidine: 0.67 nm, and 2,4,6-collidine: 0.74 nm) over hierarchical porous ZSM-5 crystals. The samples were prepared by selective silicon extraction of a commercial sample in NaOH (desilication), and they contained different degrees of intracrystalline mesoporosity. Our results demonstrate the enhanced accessibility of Brønsted acid sites in the hierarchical zeolites. For example, a relatively bulky molecule such as collidine, which probes practically no acid site of the parent medium-pore MFI structure, can access up to 40% of the acid sites in the mesoporous sample. The ACI is a powerful tool to standardize acid site accessibility in zeolites, and can be used to rank the effectiveness of synthetic strategies to prepare hierarchical zeolites.

© 2009 Elsevier Inc. All rights reserved.

1. Introduction

Zeolites are crystalline metallosilicates featuring ordered micropores (0.25–1 nm) that enable shape-selective transformations. Due to their frequent operation in the so-called transport limitation regime, the activity and occasionally also the selectivity and lifetime of zeolites in catalytic reactions are largely limited [1]. It is therefore of great importance to increase the accessibility and molecular transport to/from the active sites in zeolites to reach their full catalytic potential. During the last decade, hierarchical zeolites have emerged as an important class of materials leading to improved catalytic performance compared to their microporous parents [2]. This is due to the integration in the same material of the catalytic properties of the native micropores and the facilitated transport brought by interconnections with a secondary mesopore network of inter- or intracrystalline nature. Besides, the mesopore walls can also be catalytically active [3], widening the scope of zeolites for reactions involving bulky molecules. A number of templating and non-templating routes are available to synthesize hierarchically structured zeolites in the form of nanocrystals, nanosheets, composites, and mesoporous crystals [2,4–9].

A few studies of probe hydrocarbon molecules (neopentane, cumene, *n*-heptane, 1,3-dimethylcyclohexane, and *n*-undecane) [10–12] have demonstrated the enhanced diffusion in hierarchical ZSM-5 and ZSM-12 zeolites with respect to their purely microporous counterparts. However, an enhanced access to catalytically active sites in hierarchical zeolites has never been proven in a direct way. Therefore, no protocol exists so far to quantitatively assess the accessibility of potential active sites in microporous materials in general, and in particular of hierarchical zeolites prepared by different routes. This understanding is of key importance for rational catalyst design since it bridges materials' properties, transport, and catalytic performance.

IR spectroscopy of probe molecules (mostly pyridines, nitriles, and CO at low temperature) can be used to determine the number, strength, and location of acid sites in microporous zeolites [13–19]. The limited access of probe molecules to sterically hindered sites can be studied by infrared spectroscopy, and the strength of the H-bond with the probe is influenced in case of limited access [20]. ^{15}N NMR spectroscopy of di-tert-butylpyridine has also been used to analyze sterically unhindered acid sites in zeolites [21]. Recent work has shown that in situ UV–vis microspectroscopy and fluorescence microscopy during styrene oligomerization can assess the location and relative strengths of Brønsted acid sites in a spatially resolved manner using large zeolite crystals [22]. This approach was applied to study the effect of mesoporosity in

* Corresponding authors. Address: Institute of Chemical Research of Catalonia (ICIQ), Avinguda Països Catalans 16, 43007 Tarragona, Spain. Fax: +34 977 92 0224.
E-mail addresses: fts@ensicaen.fr, jperez@iciq.es (J. Pérez-Ramírez).

0021-9517/$ - see front matter © 2009 Elsevier Inc. All rights reserved.
doi:10.1016/j.jcat.2009.03.006

hierarchical ZSM-5 crystals prepared by desilication [23]. The above-mentioned efforts however have not yet resulted in a standardized protocol to quantify improved access in hierarchical zeolites.

Herein, infrared spectroscopy of alkylpyridines with different size (pyridine: 0.57 nm, 2,6-lutidine: 0.67 nm, and 2,4,6-collidine: 0.74 nm) and basic strength (pKa's: pyridine: 5.06, 2,6-lutidine: 6.75, and 2,4,6-collidine: 7.59) is shown to be a powerful method to quantify the remarkably enhanced accessibility of acid sites in hierarchically structured ZSM-5 (micropores of 0.56 nm) prepared by desilication. A related spectroscopic methodology was used to study the accessibility of acid sites in dealuminated mordenite prepared by acid leaching [13].

2. Experimental

2.1. Parent zeolite and treatments

A commercial ZSM-5 zeolite (Zeolyst CBV8014, NH_4-form, Si/Al ratio = 42) was used in this study. Prior to further investigation, the sample was calcined in static air at 823 K for 5 h at a heating rate of 5 K min^{-1}. Alkaline treatment of the parent zeolite was conducted in a 16-parallel reactor system (MultiMax, Mettler Toledo). The reactors (17 mm inner diameter, total volume 50 ml) were filled with 5 ml of 0.2 M NaOH aqueous solution at 318–338 K under vigorous stirring, and the zeolite (166 mg) was dispersed and treated for 30 min. The resulting suspension was cooled in an ice bath, filtered, washed until the pH was neutral, and dried at 373 K for 12 h. Finally, the alkaline-treated samples were converted into the H-form by three consecutive ion exchanges in 0.1 M aqueous NH_4NO_3 at 298 K followed by calcination in static air at 823 K for 5 h.

2.2. Characterization

The chemical composition of the samples was determined by Inductively Coupled Plasma-Optical Emission Spectroscopy (ICP-OES) (Perkin-Elmer Optima 3200RL (radial)). Powder X-ray diffraction (XRD) patterns were recorded on a Bruker AXS D8 Advance diffractometer equipped with a Cu tube, a Ge(1 1 1) incident beam monochromator (λ = 0.1541 nm), and a Vantec-1 PSD. Data were collected in the range of 5–50° 2θ with an angular step size of 0.016° and a counting time of 6 s per step. N_2 adsorption at 77 K was measured with a Quantachrome Quadrasorb-SI gas adsorption analyzer. Prior to the measurement, the samples were degassed in vacuum at 623 K for 12 h. The *t*-plot method was used to discriminate between micro- and mesoporosity. The mesopore size distribution was obtained by the BJH model applied to the adsorption branch of the isotherm. Transmission electron microscopy (TEM) was carried out with a JEOL JEM-1011 microscope operated at 100 kV and equipped with a SIS Megaview III CCD camera. A few droplets of the sample suspended in ethanol were placed on a carbon-coated copper grid followed by evaporation at ambient conditions.

2.3. Infrared spectroscopy

Infrared spectra were recorded with a Nicolet Magna 550-FT–IR spectrometer at 2 cm^{-1} optical resolution, with one level of zero-filling for the Fourier transform. Prior to the measurements, the catalysts were pressed in self-supporting discs (diameter: 1.6 cm, ~7 mg cm^{-2}) and were pre-treated in the IR cell attached to a vacuum line at 723 K for 4 h up to 10^{-6} Torr. Adsorption of substituted pyridines (pyridine (Py), 2,6-lutidine (Lu), and 2,4,6-collidine (Coll)) was performed at 300 K in successive doses of 0.3–1 μmol. At the end of each adsorption experiment, a pressure of 1 Torr was established in the cell to reach saturation followed by evacuation at 473 K to remove physisorbed species. All spectra were normalized to 10 mg wafers, and are shown in the online Supplementary material. Difference spectra were obtained by subtracting the spectrum of the zeolite before probe adsorption. The amount of adsorbed probe molecule was determined by using the integrated area of a given band with the molar extinction coefficients given in [13].

3. Results and discussion

3.1. Mesoporous zeolites

Desilication is a post-synthesis treatment involving the selective extraction of framework silicon in an alkaline medium, usually NaOH [24,25]. A commercial ZSM-5 zeolite (CBV 8014, Zeolyst) with a molar Si/Al ratio of 42 was used as the parent sample (P). The zeolite exhibits the MFI structure as the only crystalline phase and a type I N_2 isotherm (Fig. 1), confirming its microporous character. Its micropore volume (V_{micro} = 0.17 cm^3 g^{-1}) is characteristic of MFI and its mesopore surface area (S_{meso} = 58 m^2 g^{-1}) results from the crystals' external surface and surface roughness. Alkaline treatments were conducted in 0.2 M NaOH aqueous solution for 30 min at 318 K (H1), 328 K (H2), and 338 K (H3), followed by three consecutive ion exchanges with NH_4NO_3 and calcination in order to obtain the protonic form of the zeolites. Hierarchically structured zeolites with different degrees of intracrystalline meso-

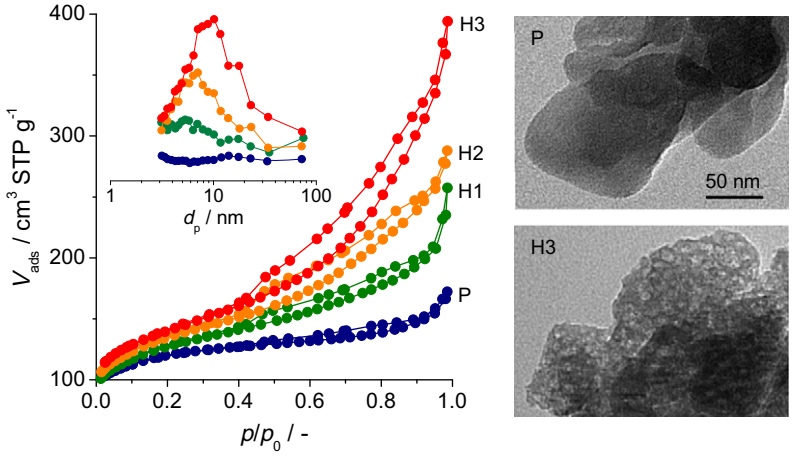

Fig. 1. N_2 isotherms and transmission electron micrographs of the parent (P) and hierarchical (H) ZSM-5 zeolites. Inset: BJH pore size distributions.

Table 1
Characterization of the zeolites and quantified infrared results with the substituted pyridines.

Sample	Si/Al[a] (mol mol^{-1})	Al[a] (μmol g^{-1})	V_{pore} (cm^3 g^{-1})	V_{micro}[b] (cm^3 g^{-1})	S_{meso}[b] (m^2 g^{-1})	S_{BET}[c] (m^2 g^{-1})	B_{Py}/Al[d] (–)	L_{Py}/Al[d] (–)	B_{Lu}/Al[d] (–)	B_{Coll}/Al[d] (–)	ACI_{Py}[e] (–)	ACI_{Lu}[e] (–)	ACI_{Coll}[e] (–)
P	42	333	0.28	0.17	58	449	0.70	0.18	0.33	0.04	0.88	0.47	0.06
H1	36	407	0.36	0.14	128	462	0.81	0.16	0.35	0.09	0.98	0.43	0.11
H2	30	482	0.43	0.12	208	486	0.53	0.34	0.30	0.08	0.87	0.57	0.15
H3	26	533	0.57	0.09	277	510	0.48	0.50	0.47	0.18	0.98	0.99	0.38

[a] ICP analysis.
[b] *t*-plot.
[c] BET method.
[d] Ratio between the amount of Brønsted (B) or Lewis (L) sites determined by pyridine (Py), lutidine (Lu), and collidine (Coll) and the amount of aluminum in the samples.
[e] Accessibility index, defined in the text.

porosity were obtained, with S_{meso} up to 277 m^2 g^{-1} (Table 1). The extra mesoporosity was created at the expense of microporosity, which decreased from 0.17 cm^3 g^{-1} in P to 0.09 cm^3 g^{-1} in H3. As a result of the selective silicon extraction, the Si/Al ratio in the resulting solids decreased from 42 to 26. As seen in Fig. 1, the original type I isotherm in the parent zeolite evolved into a combined type I and type IV isotherm, characteristic of a hierarchical porous system coupling micro- and mesoporosity. The absence of a forced closure in the hysteresis loop of the isotherms indicates the formation of accessible mesoporosity [26]. As shown in the inset of Fig. 1, the adsorption BJH pore size distributions indicate the formation of mesopores centered around 10 nm. The intracrystalline mesopores in the hierarchical zeolites can be nicely visualized by transmission electron microscopy (H3 in Fig. 1, right). In contrast, the parent zeolite (purely microporous) shows solid dark dense crystals. Despite the drastic porosity changes, the alkaline treatment did not alter the native X-ray crystallinity of the zeolites noticeably (Fig. SI1, Supplementary material). The textural characterization is substantiated by infrared spectroscopy. The spectra of the desilicated samples (Fig. SI2, Supplementary material) evidenced an increased intensity of the 3745 cm^{-1} band assigned to silanol groups. This indicates an increase of the ratio between the external and mesopore surface and the micropores' surface, the latter almost devoid of silanol groups.

3.2. Accessibility index (ACI)

Pyridine (Py), lutidine (Lu), and collidine (Coll) were adsorbed on the zeolites at 300 K followed by evacuation at 473 K in order to remove the excess of physisorbed probe molecules. Typical spectra of adsorption and desorption of the substituted alkylpyridines on the samples are shown in Figs. SI3–SI6 of the Supplementary material. Table 1 summarizes the results obtained from infrared measurements. It can be noticed that if each Al atom in the structure is responsible for either a Lewis or a Brønsted acid site, then the relative amount of potential sites detected by Py is constant. Upon desilication, the relative amount of Lewis sites in the mesoporous zeolite increases, pointing to the transformation of some of the Brønsted sites into Lewis sites. This observation is in good agreement with the recent spectroscopic studies on desilicated ZSM-5 by Holm et al. [19], and indicates an extraction of some lattice Al to extra-framework positions during the NaOH treatment.

The accessibility index (ACI) for a given molecule is defined as the number of acid sites detected by adsorption of the probe divided by the total amount of acid sites in the zeolite based on the measured aluminum content. Accessibility for pyridine is thus $ACI_{Py} = (B_{Py} + L_{Py})/n\mathrm{Al}$, as Py probes both Brønsted and Lewis sites. Since pyridine can reach most of the acid sites in the MFI structure, its ACI amounts to ca. 1 for all zeolites, including the parent material. Lu and Coll only probe Brønsted sites in the samples, therefore the corresponding ACI can be defined as the ratio between the number of Brønsted sites they detect and the total number of Brønsted sites (i.e. the number of Brønsted sites probed by Py). Fig. 2 plots the accessibility index of the different probe molecules as a function of the mesopore surface area generated by desilication. As stated above, pyridine probes a large fraction of the acid sites on the parent material. Lutidine being significantly bigger than pyridine probes <50% of the sites on the parent material. Collidine is clearly too bulky to enter the ZSM-5 micropores, and reaches nearly no sites in the purely microporous zeolite. Upon enhancing the mesopore surface area by desilication, only a slight increase in the ACI of pyridine is observed as the molecule accesses most of the acid sites in the parent zeolite. However, the accessibility indexes increased for larger probe molecules. The enhanced accessibility is spectacular for H3, i.e. the sample with the highest S_{meso}. ACI(Lu) reaches the maximum value of 1, while ACI(Coll) increases from 0 to 0.4.

A straightforward infrared spectroscopic method, widely available to the catalysis community, demonstrates for the first time in an unequivocal and quantitative manner the enhanced accessibility of acid sites in mesoporous zeolites prepared by desilication. It can be directly related to their improved catalytic performance in many reactions [2]. The accessibility index (ACI) of the probe molecules correlates with the mesopore surface area of the hierarchical zeolites. The creation of mesoporosity in the zeolite crystals shortens the average length of the micropores (diffusion distance), and also leads to an increase of the available active sites at the pore mouths, which are accessible both to lutidine and to collidine. Our results support the previous work by the group of Ryoo [3], in which the mesoporous walls of hierarchical zeolites prepared by supramolecular templating were found to be catalytically active in reactions involving bulky molecules.

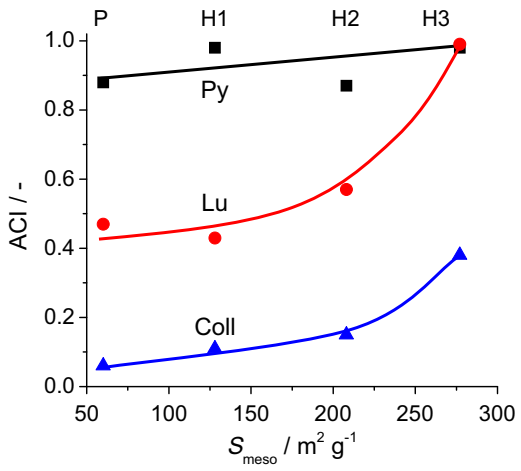

Fig. 2. Accessibility index (ACI) of pyridine, lutidine, and collidine versus the mesopore surface area of the ZSM-5 zeolites.

The characterization of the accessibility of catalytic sites in porous solid acids has been monitored often by infrared spectroscopy, but the ACI quantifies and standardizes site accessibility in zeolites. Pore systems other than that of MFI can be studied using smaller probe molecules than pyridine, for example, substituted nitriles [14–16]. The ACI can be used to rank the effectiveness of synthetic strategies toward hierarchical zeolites (nanocrystals, composites, and mesoporous crystals). The ACI method goes therefore beyond the primary assessment of samples by measuring their mesopore surface area by gas adsorption analyses. The protocol introduced here provides information not only on the quantity but also on the quality of the mesoporosity introduced. Finally, the methodology is not specimen dependent, i.e. it can be equally applied to commercial zeolites of nanocrystalline nature as well as to nicely grown zeolite crystals. The influence of desilication on the strength of the acid (Brønsted and Lewis) sites is best studied by low temperature adsorption monitored by CO [16,19,27], and it is not the object of the present communication. Further studies are underway to link ACI with the effectiveness factor, i.e. the number of sites actually involved in a catalytic reaction. This will lead to true turnover frequencies, enabling reliable comparison of catalytic data by different research groups.

Acknowledgments

This work was supported by the Spanish MEC (CTQ2006-01562/PPQ, PTQ05-01-00980, and Consolider-Ingenio 2010 Grant CSD2006-0003), the ICIQ Foundation, and the Région Basse-Normandie.

Appendix A. Supplementary material

Supplementary data associated with this article can be found, in the online version, at doi:10.1016/j.jcat.2009.03.006.

References

[1] A. Corma, Chem. Rev. 97 (1997) 2373.
[2] J. Pérez-Ramírez, C.H. Christensen, K. Egeblad, C.H. Christensen, J.C. Groen, Chem. Soc. Rev. 37 (2008) 2530, and references therein.
[3] V.N. Shetti, J. Kim, R. Srivastava, M. Choi, R. Ryoo, J. Catal. 254 (2008) 296.
[4] A. Corma, U. Diaz, M.E. Domine, V. Fornés, Angew. Chem. Int. Ed. 39 (2000) 1499.
[5] S. van Donk, A.H. Janssen, J.H. Bitter, K.P. de Jong, Catal. Rev. Sci. Eng. 45 (2003) 297.
[6] L. Tosheva, V.P. Valtchev, Chem. Mater. 17 (2005) 2494.
[7] Y. Tao, H. Kanoh, L. Abrams, K. Kaneko, Chem. Rev. 106 (2006) 896.
[8] J. Čejka, S. Mintova, Catal. Rev. Sci. Eng. 49 (2007) 457.
[9] K. Egeblad, C.H. Christensen, M. Kustova, C.H. Christensen, Chem. Mater. 20 (2008) 946.
[10] J.C. Groen, W. Zhu, S. Brouwer, S.J. Huynink, F. Kapteijn, J.A. Moulijn, J. Pérez-Ramírez, J. Am. Chem. Soc. 129 (2007) 355.
[11] X. Wei, P.G. Smirniotis, Micropor. Mesopor. Mater. 89 (2006) 170.
[12] L. Zhao, B. Shen, J. Gao, C. Xu, J. Catal. 258 (2008) 228.
[13] N.S. Nesterenko, F. Thibault-Starzyk, V. Montouillout, V.V. Yuschenko, C. Fernandez, J.-P. Gilson, F. Fajula, I.I. Ivanova, Micropor. Mesopor. Mater. 71 (2004) 157.
[14] S. van Donk, E. Bus, A. Broersma, J.H. Bitter, K.P. de Jong, J. Catal. 212 (2002) 86.
[15] T. Montanari, M. Bevilacqua, G. Busca, Appl. Catal. A 307 (2006) 21.
[16] G. Busca, Chem. Rev. 107 (2007) 5366.
[17] B. Gil, S.I. Zones, S.-J. Hwang, M. Bejblova, J. Čejka, J. Phys. Chem. C 112 (2008) 2997.
[18] V.V. Ordomsky, V.Y. Murzin, Yu.V. Monakhova, Y.V. Zubavichus, E.E. Knyazeva, N.S. Nesterenko, I.I. Ivanova, Micropor. Mesopor. Mater. 105 (2007) 101.
[19] M.S. Holm, S. Svelle, F. Joensen, P. Beato, C.H. Christensen, S. Bordiga, M. Bjørgen, Appl. Catal. A 356 (2009) 23.
[20] B. Onida, B. Bonelli, L. Borello, S. Fiorilli, F. Geobaldo, E. Garrone, J. Phys. Chem. B 106 (2002) 10518.
[21] D. Farcasiu, R. Leu, A. Corma, J. Phys. Chem. B 106 (2002) 928.
[22] M.H.F. Kox, E. Stavitski, B.M. Weckhuysen, Angew. Chem. Int. Ed. 46 (2007) 3652.
[23] M.H.F. Kox, E. Stavitski, J.C. Groen, J. Pérez-Ramírez, F. Kapteijn, B.M. Weckhuysen, Chem. Eur. J. 14 (2008) 1718.
[24] J.C. Groen, L.A.A. Peffer, J.A. Moulijn, J. Pérez-Ramírez, Chem. Eur. J. 11 (2005) 4983.
[25] J.C. Groen, J.A. Moulijn, J. Pérez-Ramírez, J. Mater. Chem. 16 (2006) 2121.
[26] J.C. Groen, L.A.A. Peffer, J. Pérez-Ramírez, Micropor. Mesopor. Mater. 60 (2003) 1.
[27] J.A. Lercher, C. Grundling, G. Edermirth, Catal. Today 27 (1996) 353.